

## **Electronic Supplementary Information for “Ultrafast Al(Si)-Induced Crystallisation Process At Low Temperature”**

Sung-Yen Wei,<sup>a</sup> Sheng-Min Yu,<sup>b</sup> Li-Chi Yu,<sup>a</sup> Wen-Ching Sun,<sup>b</sup> Chien-Kuo Hsieh,<sup>a</sup> Tzer-Shen Lin,<sup>b</sup> Chuen-Horng Tsai,<sup>a</sup> and Fu-Rong Chen\*<sup>a</sup>

<sup>a</sup> Department of Engineering and System Science, National Tsing Hua University, Hsinchu 30033, Taiwan, R.O.C

<sup>b</sup> Material and Chemical Research Laboratories ,Industrial Technology Research Institute, Chutung, Hsinchu 31040, Taiwan, R.O.C

\* E-mail: [frchen@ess.nthu.edu.tw](mailto:frchen@ess.nthu.edu.tw)

Fax: (+886)-3 -5734066

Tel: (+886)-3 -5715131 Ext. 62247

## 1. The Schematic diagram of AIC process<sup>1,2</sup>

The basic model of aluminium-induced crystallization process can be presented as

Fig. S1:

- (1) Si atoms diffused into the Al film through a thin  $\text{Al}_2\text{O}_3$  permeable membrane between the initial Al and a-Si layers.
- (2) Silicon diffuses within the Al layer.
- (3) Silicon nuclei are formed within the Al layer and grow in all directions until confined within the Al layer between glass substrate and Al oxide layer.
- (4) After confinement the silicon grains grow laterally until neighboring grains form a continuous poly-Si film on the glass substrate.
- (5) Al is displaced and diffuses across the Al oxide interface into the initial a-Si layer.

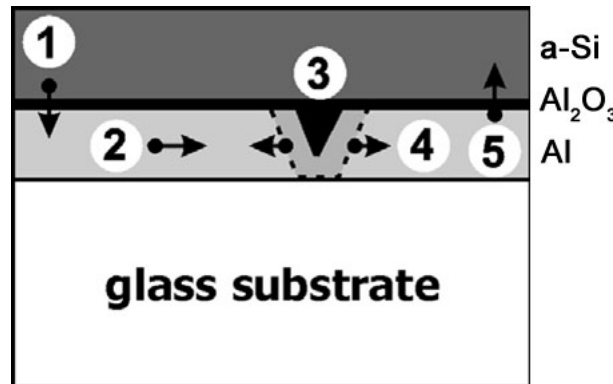


Figure S1. The basic model of aluminium-induced crystallisation process.

## 2. Optical microscope image of sample A and B

Samples A and B was prepared by stack of pure-Al/native- $\text{Al}_2\text{O}_3$ /a-Si and Si-doped/native- $\text{Al}_2\text{O}_3$ /a-Si, respectively. After annealing under 673K for 6 min and 5 hours, samples A and B were both observed by optical microscope through the glass side. As shown in Fig. S2(a), the dark regions were the nuclei of c-Si,

which indicated that the AIC reaction of sample A was just started whilst annealing under 673K for 6 minutes. After 5 hours annealing the reaction was completed with forming continuous c-Si film, as in Fig. S2(b). In contrast with sample A, the reaction of sample B was fast completed after 673K /6min annealing (Fig. S2(c)), and was with no difference whilst extending the annealing duration to 5 hours (Fig. S2(d)).

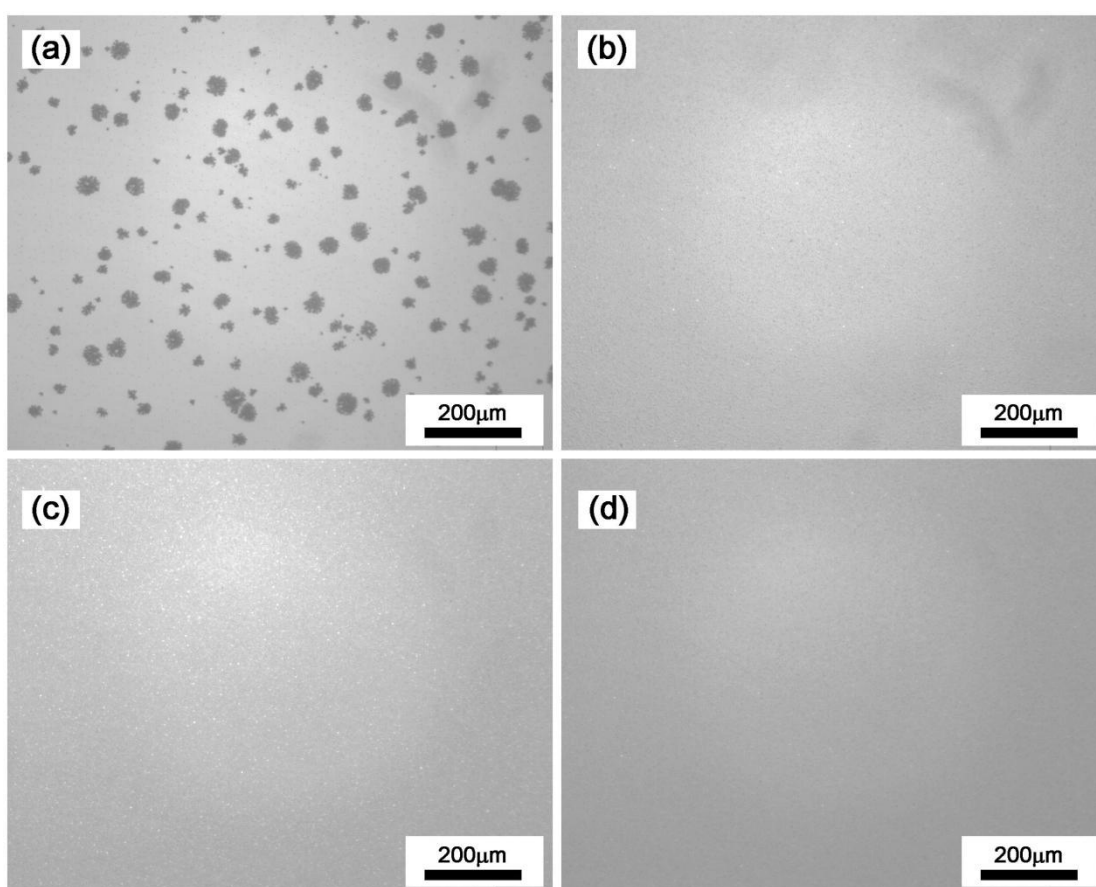


Figure S2. Optical microscope images of sample A annealed under 673K for (a) 6 minutes and (b) 5 hours. Sample B annealed under 673K for (a) 6 minutes and (b) 5 hours.

### 3. High resolution TEM analysis of interlayer Al<sub>2</sub>O<sub>3</sub> membrane

The native Al<sub>2</sub>O<sub>3</sub> membranes of pure-Al and Si-doped-Al were analyzed by high resolution TEM. As shown in Fig. S3(a)(b), the thickness of native oxide of

pure-Al and Si-doped-Al were about 2.12 nm and 2.08 nm, respectively. The uniform oxide layers of both pure-Al and Si-doped-Al were observed, and almost the same thickness of these native oxide layers indicated that 1% Si doped in Al will affect the native oxide formation limitedly. As a diffusion barrier, doping 1%Si in Al layer will not make any influence on inter-diffusion of Al/Si by interlayer oxide thickness.

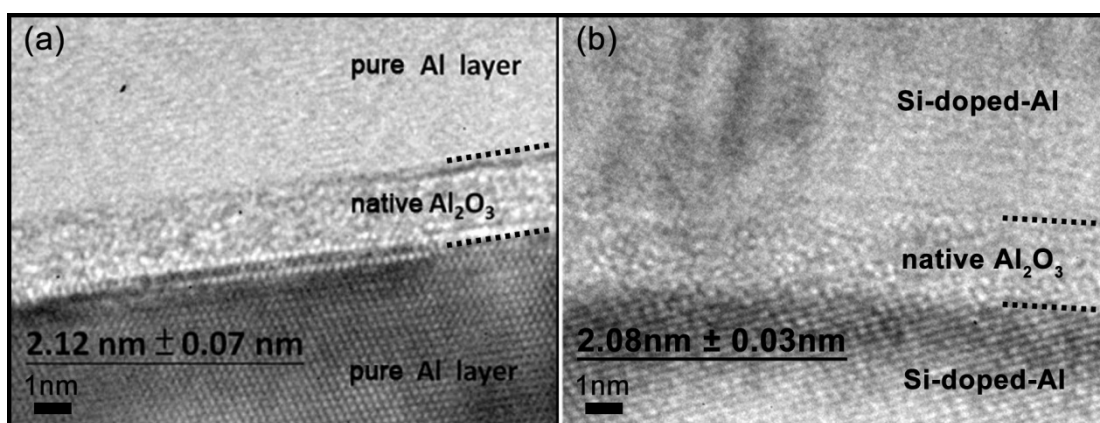


Figure S3. High resolution TEM of native oxide layers of (a) pure-Al and (b) Si-doped-Al.

#### 4. Thermodynamics calculation of homo-/heterogeneous nucleation

The free energy of homogeneous nucleation could be presented by

$$\Delta G^{homo} = \frac{4}{3}\pi r^3 \frac{\Delta g^{vl}}{v_l} + 4\pi r^2 \gamma_{<Al>|<Si>}^{interface} \quad (1)$$

Where

$\Delta G^{homo}$ : Free energy of homogeneous nucleation,

$r$ : Radius of c-Si nucleus,

$\Delta g^{vl}$ : Volume free energy per Si atom,

$v_l$ : Volume of a Si atom in crystalline Si matrix,

$\gamma_{<Al>|<Si>}^{interface}$ : Interfacial energy of crystalline Al and crystalline Si contact.

The free energy of heterogeneous nucleation could be presented by

$$\Delta G^{het-top} = V_c \Delta g_v + A_{<Al>|<Si>} \gamma_{<Al>|<Si>}^{interface} + A_{\{Al_2O_3\}|<Si>} (\gamma_{\{Al_2O_3\}|<Si>}^{interface} - \gamma_{\{Al_2O_3\}|<Al>}^{interface}) \quad (2)$$

$$\Delta G^{het-bottom} = V_c \Delta g_v + A_{<Al>|<Si>} \gamma_{<Al>|<Si>}^{interface} + A_{\{SiO_2\}|<Si>} (\gamma_{\{SiO_2\}|<Si>}^{interface} - \gamma_{\{SiO_2\}|<Al>}^{interface}) \quad (3)$$

Where

$\Delta G^{het-top}$ : Free energy of heterogeneous nucleation at top interface ( $Al_2O_3/Al$ ),

$\Delta G^{het-bottom}$ : Free energy of heterogeneous nucleation at bottom interface

( $SiO_2/Al$ )

$V_c$ : is the volume of crystalline Si,

$\Delta g_v$ : Volume crystallization free energy of Si,

$A_{<Al>|<Si>}$ : Contact area between crystalline Al and crystalline Si,

$A_{\{Al_2O_3\}|<Si>}$ : Contact area between amorphous  $Al_2O_3$  and crystalline Si,

$A_{\{SiO_2\}|<Si>}$ : Contact area between glass and crystalline Si,

$\gamma_{\{Al_2O_3\}|<Si>}^{interface}$ : Interfacial energy of amorphous  $Al_2O_3$  and crystalline Si,

$\gamma_{\{Al_2O_3\}|<Al>}^{interface}$ : Interfacial energy of amorphous  $Al_2O_3$  and crystalline Al,

$\gamma_{\{SiO_2\}|<Si>}^{interface}$ : Interfacial energy of glass and crystalline Si

$\gamma_{\{SiO_2\}|<Al>}^{interface}$ : Interfacial energy of glass and crystalline Al

Or also, the free energy of heterogeneous nucleation could be a relation of contact angle of c-Si nucleus and free energy of homogeneous nucleation as below:

$$\Delta G^{het} = \Delta G^{homo} \frac{(2-3\cos\theta+\cos^3\theta)}{4} \quad (4)$$

These interfacial energies we calculated here could be found in several literatures.<sup>3-6</sup>

From equations above the free energy was a function of c-Si nucleus radius, the critical radius of c-Si nucleation could be found at about 0.84nm as shown in Fig. S4(a). The Fig. S4(b) is the cross-sectional TEM analysis of c-Si nucleus at the upper and bottom interfaces. As in the calculation of the free energy of nucleation, the free energy requirement of heterogeneous nucleation was only about half of homogeneous nucleation at the critical radius, which indicated that the homogeneous nucleation was difficult to occur in the general AIC process.

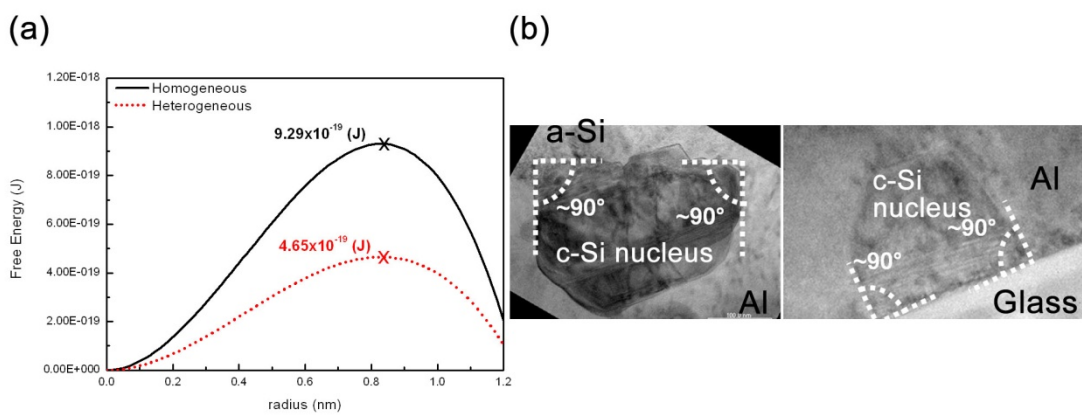


Figure S4. (a) The free energy versus radius of nucleus. (b) the contact angle of nuclei in Si-doped-Al AIC process.

## 5. Arrhenius-type behaviour for the grain growth process of conventional AIC process.

The activation energy was calculated according to the relationship  $V_g = Ae^{-E_a/RT}$ , where  $V_g$  is the grain growth rate, A is the frequency factor,  $E_a$  is the activation energy, R is the Boltzmann constant, and T is the absolute temperature. Fig. S5 shows the grain size as a function of annealing time at various temperatures. As shown in the inset of Fig. S5, the activation energy can be determined to be around 1.86eV, which is obtained from the plot of  $\ln(V_g)$  versus  $1000/T$ .

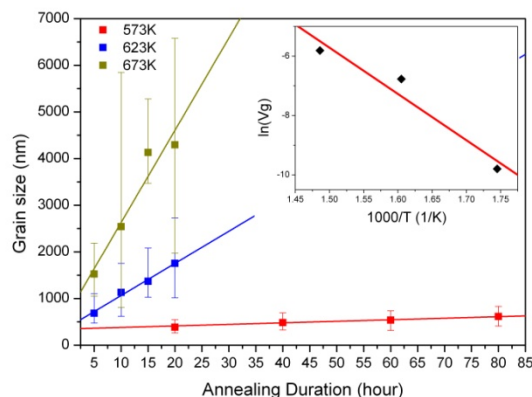


Figure S5. Grain growth rate measurement at annealing temperatures of 573K, 623K and 673K for Arrhenius behaviour analysis (inset) of sample A.

## Reference

1. A. Sarikov, J. Schneider, J. Klein, M. Muske and S. Gall, *Journal of Crystal Growth*, 2006, **287**, 442-445.
2. J. Schneider, J. Klein, A. Sarikov, M. Muske, S. Gall and W. Fuhs, Symposium on Amorphous and Nanocrystalline Silicon Science and Technology held at the 2005 MRS Spring Meeting, San Francisco, CA, 2005.
3. Z. M. Wang, L. Gu, F. Philipp, J. Y. Wang, L. P. H. Jeurgens and E. J. Mittemeijer, *Advanced Materials*, 2011, **23**, 854-+.
4. Z. M. Wang, L. P. H. Jeurgens, J. Y. Wang and E. J. Mittemeijer, *Advanced Engineering Materials*, 2009, **11**, 131-135.
5. F. Sommer, R. N. Singh and E. J. Mittemeijer, *Journal of Alloys and Compounds*, 2009, **467**, 142-153.
6. L. P. H. Jeurgens, Z. M. Wang and E. J. Mittemeijer, *International Journal of Materials Research*, 2009, **100**, 1281-1307.